Evaluation of the Storm Surge Hazard in Coastal Mississippi

A. Niedoroda[1], D. Resio[2], G. Toro[3], D. Divoky[4], H. Das[1], C. Reed[1]

[1] *URS Corporation, 1625 Summit Lake Drive, Suite 200,, Tallahassee, FL, 32317, USA*
[2] *U.S. Army Corps of Engineers, ERDC-CHL, 3909 Halls Ferry Rd., Vicksburg, MS 39180, USA*
[3] *Risk Engineering Inc., 3 Farmers Row, Acton, MA, 01720, USA*
[4] *Watershed Concepts, 2835 Brandywine Road, Suite 102, Atlanta, GA, 30341, USA*

Introduction

In 2004 the Federal Emergency Management Agency (FEMA) initiated a program to update the flood insurance rate maps for the state of Mississippi. The enormous devastation caused by Hurricane Katrina brought this program into sharp focus. It was clear that all of the maps in the coastal zone needed to be updated as expeditiously as possible to help promote recovery efforts.

Hurricanes Katrina and Rita also galvanized related efforts aimed at coastal Louisiana. FEMA assigned the task of restudying the Mississippi coastal areas to a team led by the URS Corporation, and directed it to work closely with similar efforts of the U.S. Army Corps of Engineers (Corps) already underway in the region. The project teams worked together sharing data and ideas.

The purpose of this paper is to describe the Mississippi Coastal Flooding Hazard Project, covering both the development of new methods and their application.

Approach

Basis of Analysis

The paucity of gage data and the scale and extent of coastal storm surges defeat attempts to characterize them by a statistical analysis of direct measurements. Tide and river gages are not adequately distributed and post-event coastal high water mark surveys are available for only a limited number of historic events. Accordingly, it is necessary to perform simulation studies using knowledge of the local climatology combined with numerical models capable of accurately simulating hurricane storm surges throughout the coastal zone. A variety of model frameworks are available; for this work, an updated and highly efficient version of the Joint Probability Method (JPM) was developed and applied.

The analysis is based on the assumption that future storm conditions and their related coastal floods will be statistically similar to past conditions, and so requires a good characterization of historical storm conditions in the project area. But hurricanes, especially great ones, are rare events, making the characterization of the storm climatology a challenging undertaking.

Project Components

The study can be divided into six major components, as follows:

- Characterization of the local hurricane climatology
- Establishment of a representative set of synthetic storms for simulation
- Numerical simulation of the synthetic storms and their storm surges
- Statistical characterization of the coastal flooding levels
- Inclusion of additional effects of waves and wave heights

- Mapping of the coastal flood zones

Data Sources

The major sources of storm data were: the National Oceanic and Atmospheric Administration (NOAA) Atlantic basin hurricane database (HURricane DATabase or HURDAT); NOAA Technical Report NWS 38, Hurricane Climatology for the Atlantic and Gulf Coasts of the United States (Ho *et al*. 1987); NOAA Technical Memo NWS TPC-4 (Blake *et al.* 2006); NOAA Technical Memo NWS TPC-1 (Hebert *et al*. 1996); and the National Hurricane Center Tropical Cyclone reports for individual storms. Other sources included: NOAA and U.S. Air Force hurricane hunter aircraft measurements, NHRD HWind analyses, NOAA buoy and C-MAN stations, composite NWS radar imagery, Doppler radar PBL flow velocity estimates, NOAA GOES visual, infrared, and water vapor imagery, NCEP model wind fields, QUIKSCAT scatterometer winds, and TOPEX altimeter winds and waves.

Other sources provided additional information for Hurricanes Camille and Betsy. These included the USACE Mobile District Hurricane Camille Report (May 1970); the reports by Hamilton and Steere (1969) and Oceanweather Inc. (2007); and the papers by Goudeau and Conner (1968), Frank (1970), and Simpson *et al.* (1970).

The Suite of Numerical Models

The model suite consisted of the Planetary Boundary Layer Model (TC-96) to simulate the translating wind and pressure fields of hurricanes (Thompson and Cardone 1996); the WAM ocean wave model (Uniwave 3G) for deep-water waves, the SWAN model (ver. 40.51) for storm waves approaching the coast (Rogers et al. 2002); and the ADCIRC hydrodynamic model (ver46.52.03) for simulations of the storm surges (Westerink and Luettich 1991).

Where appropriate, alternative methods and assumptions were developed and tested using the NOAA SLOSH Model as a highly efficient diagnostic tool. SLOSH includes both hurricane and storm surge simulations, accurately capturing the major features of the surge; it does not, however, include the additional effects of storm waves.

Hurricane Climatology

Storm Parameters

In the JPM approach, storms are characterized parametrically, with the probability of a particular storm (a particular combination of the parameters) being defined by the observed statistics of those parameters. Since surge simulations using the high resolution Mississippi ADCIRC grid are computationally demanding, it is mandatory that the number of simulations be kept to an acceptable minimum. To this end, three classes of parameters were defined. The major parameter class included the central pressure deficit, storm radius, track azimuth, forward speed, and landfall position. All of these were treated by systematic variation over representative ranges of values. The second class consisted of Holland’s B parameter for which a single pattern of variation was adopted. It has been found that in the north-central Gulf of Mexico, the B tends to be similar from storm to storm, and to vary spatially in a characteristic way (Resio 2007). According to that study, B tends to vary from about 1.0 to about 1.27 in passing from 90 miles offshore to landfall. This behavior was observed for most storms having a radius to maximum winds larger than 10 nm.

The third class of storm parameters accounts for the variability in the surge due to processes and effects that are not resolved in the modeling. These include random departures of real storms from the idealized PBL behavior; lack of hydrodynamic modeling accuracy despite high resolution and detailed physics; and random coincidence between surge and the varying astronomic tide.

A series of sensitivity tests were run using the SLOSH model to assess the variation of computed surge levels versus variations in the five major storm parameters. A set of 147 diagnostic points were distributed along the coast, in coastal valleys and lowlands, and across uplands, representing major topographic features. The tests showed that central pressure deficit, proximity to the landfall point, and the storm radius exercised considerably more control on the surge response than did track azimuth and forward speed.

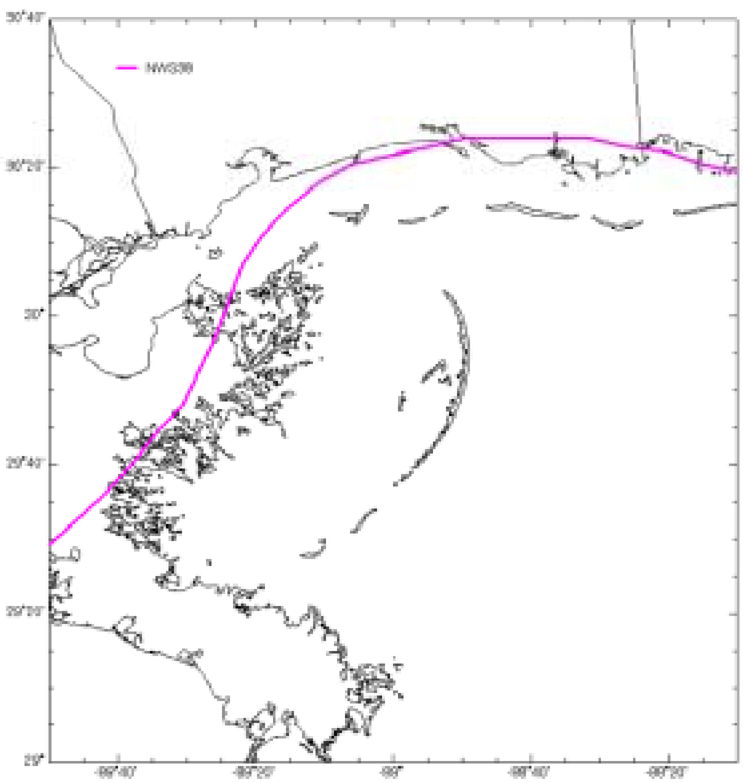

Figure 1. The simplified project shoreline.

Period of Record

Based on the considerations of data quality, the period of record was taken to be the 67 year span from 1940 through 2006. Although the HURDAT database includes information back to 1851, much of the older data is suspect and very little of it applies to offshore conditions. Aircraft observations within hurricanes started during World War II. These provided systematic measurements of storms while offshore in the Gulf of Mexico. After the initiation of these hurricane hunter flights, the quality of storm data has steadily improved as satellites, ocean data buoys, Doppler radar, and other measurement systems have been introduced.

Simplified Project Shoreline

A version of the simplified shoreline given in NWS 38 was adopted as a reference for track characterization. This is a smooth curve ignoring many of the unimportant details of the actual shoreline, the most significant departure being the truncation of the Mississippi River birdfoot delta. By eliminating this low-lying wetland feature (small compared to the size of the storms), ambiguity in landfall point is avoided; the simplified project shoreline is shown in Figure 1.

Storm Sample

Because hurricanes, especially powerful ones, are rare events with widely varying behaviors, it is difficult to characterize the local population from the local sample. One wishes to accept data from a large area in order to minimize sample error, but must restrict the range in order to minimize population error.

The Mississippi Coastal Flood Hazard Project applied a method originally introduced by Chouinard and Liu 1997, (also see Chouinard, 1992) to determine the local storm rate (storms/km yr) and the pressure deficit distribution. Input data were taken from a regional zone extending to either side of a Mississippi coastal reference point (CRP). These data were taken from storms making landfall between 85 W and 95 W in the interval from 1940 and 2006. The Chouinard method determines an optimal kernel size and weights storm data according to distance to the CRP.[1] The kernel width selected for storm density and central pressure determinations was 200 km; for track azimuth, the kernel width was 30 degrees. A total of 33 major storms were used in the characterization of the hurricane climatology. The analysis was split into two parts (in order to permit an early estimate of the extreme flood levels), corresponding to storms with pressure deficits exceeding 48 mb, and those between 31 and 48 mb. These are referred to as the greater and lesser storm sets, respectively; Of the 33 storms, 15 were in the greater storm category, which dominated surge at the 1 % annual occurrence level and above.

Storm Rate

The storm rate, or spatio-temporal density, for the greater storms was found to be 2.88E-4 storms per kilometer per year, while the rate for the lesser storms is 2.57E-4 storms per kilometer per year. These can be added to obtain a combined rate of 5.45E-4 storm/km/yr for all storms in the region having a central pressure deficit of 31mb or more.

Track Azimuth

The analysis showed that the storm path heading at landfall could be well-fitted with a Beta distribution for the greater storms and a normal distribution for the lesser storms. The mean path was directed about 10 to 12 degrees west of north, for the greater and lesser storms, respectively. These distributions are illustrated in Figures 2 and 3.

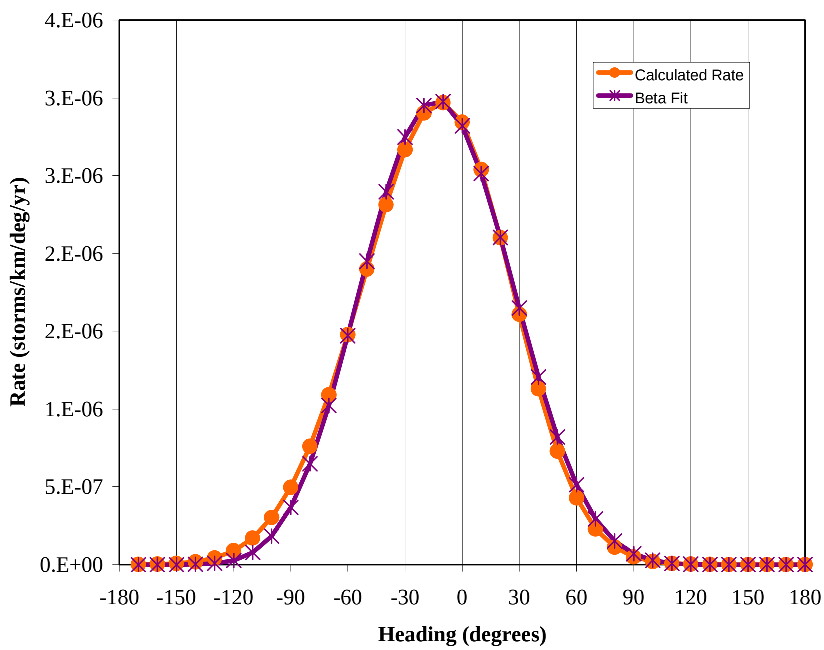

Figure 2. Directional rates and Beta distribution of storm heading for the greater storms ($\Delta P > 48$ mb).

Central Pressure Deficit

The Chouinard method was also used for the central pressure deficit, based on data from the sources identified earlier. Some inconsistencies in reported pressure values were resolved by a detailed storm-by-storm

[1] The application of the Chiounard method in the Mississippi Coastal Flood Hazard Project is described in detail in a project report by Toro (2007).

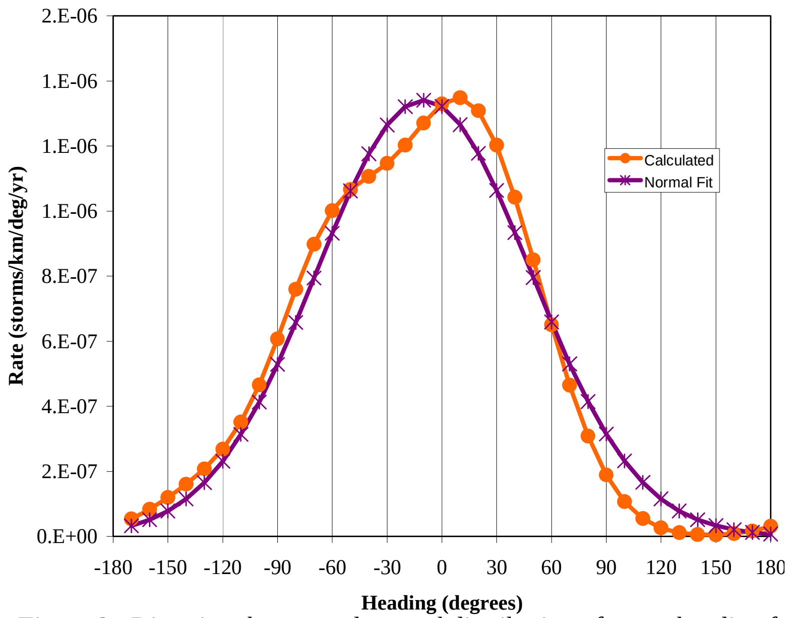

Figure 3. Directional rates and normal distribution of storm heading for the lesser storms ($31\text{mb} < \Delta P \leq 48\text{mb}$).

Central Pressure Deficit

The Chouinard method was also used for the central pressure deficit, based on data from the sources identified earlier. Some inconsistencies in reported pressure values were resolved by a detailed storm-by-storm review. The analysis showed that the local distribution of pressure deficit could be satisfactorily represented by a two-parameter Weibull Distribution. The distributions for the greater and lesser families are shown in Figures 4 and 5.

Pressure Scale Radius

There is considerable uncertainty about the degree to which the storm size (the pressure scale radius) and the central pressure deficit is statistically correlated. The data are very sparse, and relationships may be confounded by secondary factors. A review of data for hurricanes at the time of landfall in the north-central Gulf of Mexico shows no obvious relationship between these parameters. However, a larger sample of storms from the entire Gulf of Mexico does indicate that the pressure scale radius is inversely correlated with the pressure deficit. The trend suggested by the larger sample was used to define the conditional distribution of storm radius for the greater storms, given the pressure deficit; the relationship is illustrated with Figure 6.

However, this relationship tends to over-predict the pressure radius when applied to the lesser storms. Consequently, a second representation of the relationship between radius and pressure deficit was developed using data from 1950 and 2006 (Figure 7). This provided agreement with the trend adopted for the greater storms (which control 1% or 100-yr conditions), and provides more realistic radii for the lesser storms. The conditional distributions of $R_p|\Delta P$ were represented as lognormal functions.

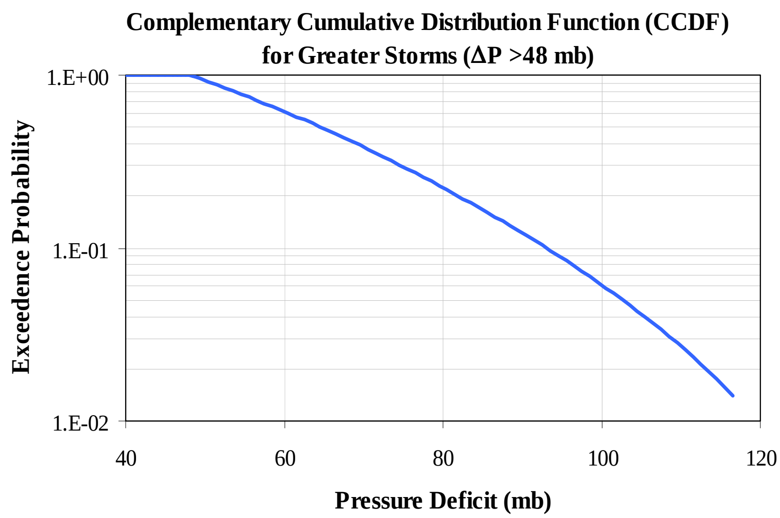

Figure 4. Probability distribution of DP for greater storms.

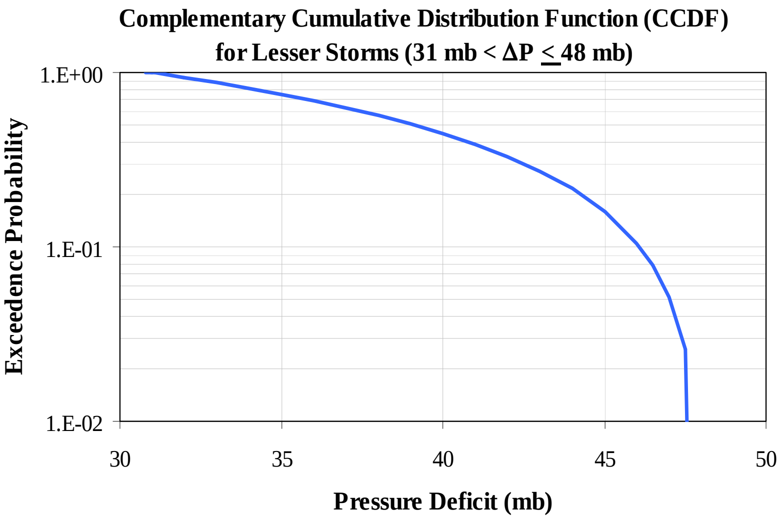

Figure 5. Probability distribution of DP for lesser storms.

Forward Speed

The forward speed of the 30 storms at the time of landfall was determined by comparing their recorded positions in the six-hour intervals bracketing the shoreline position. The data for both the greater and lesser storms were well approximated by lognormal distributions. The distributions are illustrated in Figures 8 and 9.

Storm Tracks

A series of sensitivity tests were carried out with the full PBL-WAM-SWAN-ADCIRC model suite to investigate the distance from shore over which the surge develops. As a result of these tests, it was concluded that the surge simulations should commence 3 ½ days before landfall (in addition to a 3-day model spin-up time, to establish antecedent conditions including freshwater inflow). Because wave set-up was to be resolved explicitly in the hydrodynamic simulations of each storm (rather than being treated as a separate add-on) the PBL-WAM modeling involved whole-Gulf simulations. Three families of curved tracks similar to those developed for the Corps IPET and LaCPR studies were used; the rationale for these is given in Resio (2007).

Landfall

As expected, the storm surge is usually greatest in the vicinity of the greatest winds, and so occurs about one storm radius to the right of the landfall point; the surge height usually diminishes rapidly to either side of that point. Consequently, the model simulations need to include a large number of synthetic storm tracks to properly represent

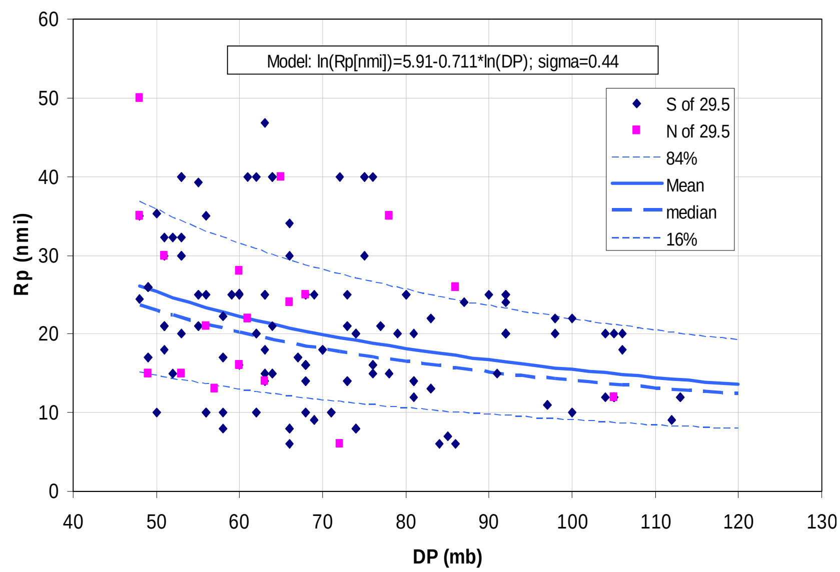

Figure 6. Data and regression for R_p vs. ΔP for greater storms using all Gulf of Mexico data.

conditions across the length of the Mississippi coast. A separate sensitivity study was conducted using SLOSH to establish the optimum spacing between these synthetic storms, balancing the need to obtain accurate results and to minimize the number of very lengthy hydrodynamic simulations. This sensitivity analysis showed that the perpendicular spacing of tracks should be approximately equal to the

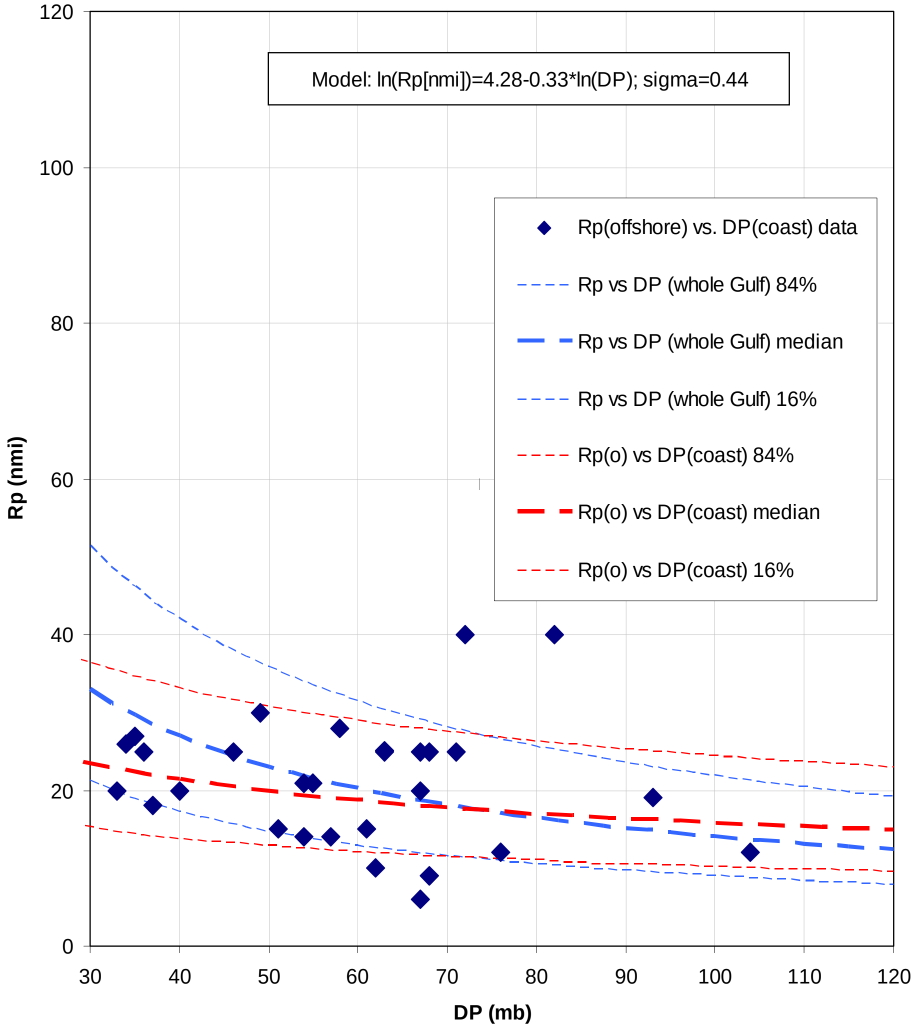

Figure 7. Data and regression for R_p (offshore) vs. ΔP (coast) for lesser and greater storms using all Gulf of Mexico data. The whole-Gulf percentile curves obtained earlier for the greater storms (Figure 6) are also shown.

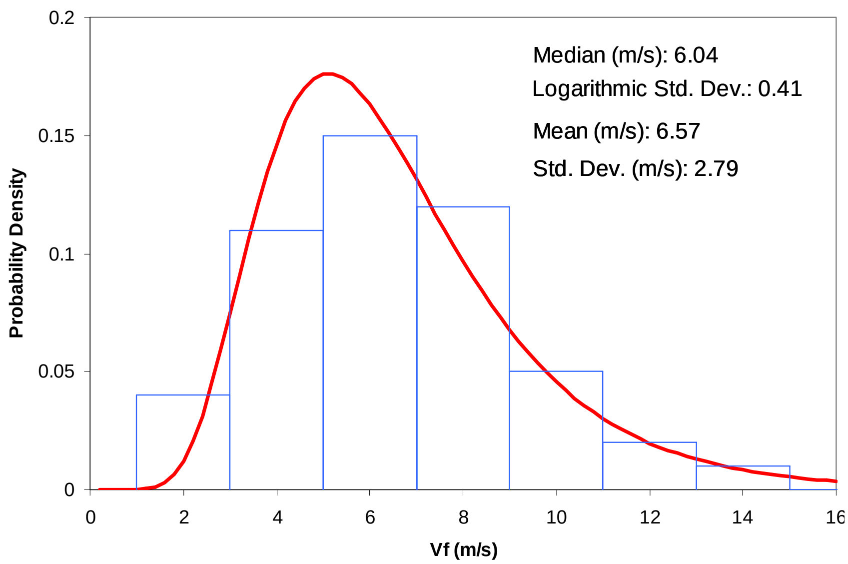

Figure 8. Distribution of forward velocity Vf at landfall for the greater storms. The histogram indicates the observed values; the smooth curve indicates the lognormal model fit.

radius to maximum winds. It also showed that the track layout for a given radius should extend at least one storm track to the east of Mississippi, and three to the west, and confirmed the desirability of randomly shifting the track origin for each radius.

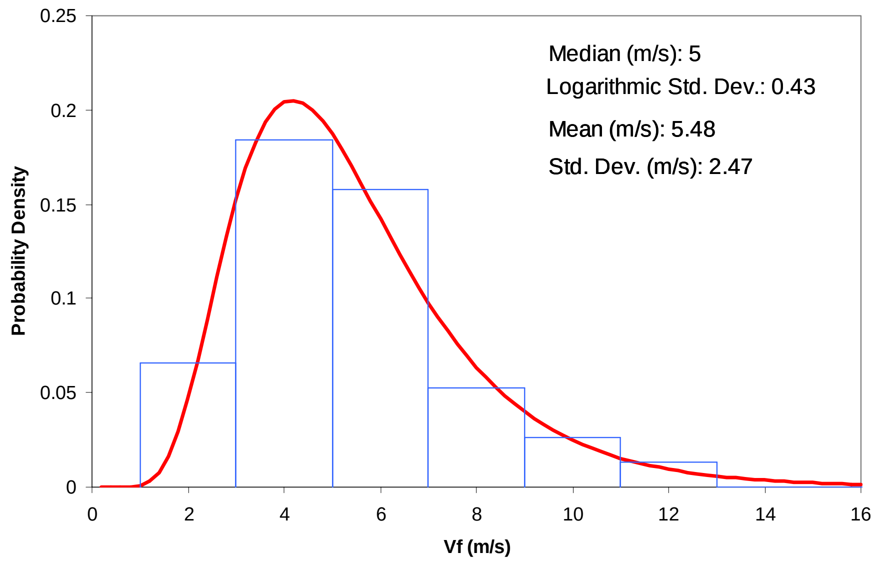

Figure 9. Distribution of forward velocity Vf at landfall for the lesser storms. The histogram indicates the observed values; the smooth curve indicates the lognormal model fit.

Method for Statistical Projection

Choice of Method

The adopted approach was based on the JPM method that has been widely used in coastal flood studies by NOAA (Myers 1975, Ho and Meyers 1975), FEMA, and others for many years. Other approaches were initially considered, including Monte Carlo (MC) methods and the Empirical Simulation Technique (EST: Borgman et al. 1992, Scheffner et al. 1993). Monte Carlo methods are generally inefficient for determination of extremes, and so were not pursued. An EST approach was initially considered for this project, but JPM was chosen after coordination with both the Corps and FEMA officials, and after it was determined that a JPM implementation could be optimized so as to eliminate the perceived computational advantage of EST.

An optimized JPM approach was formulated by Resio (2007) involving the construction of a response surface based upon a relatively small number of storm simulations. That work indicated that a very great computational savings could be achieved over older JPM studies while maintaining accuracy. The procedure was termed JPM-OS, for Optimal Sampling. The approach used in this Mississippi study is in the same OS spirit, but differs in detail.

In the JPM approach, the conditional probability that a storm with parameters $\underline{x}$ will generate a flood elevation exceeding η at a particular point can be expressed as:

$$P[\eta_{\max(1\,yr)} > \eta] = \lambda \int \ldots \int_{\underline{x}} f_{\underline{X}}(\underline{x}) P[\eta(\underline{x}) > \eta] d\underline{x} \qquad (1)$$

where λ is the mean annual rate of storms of interest for that site, $f_{\underline{X}}(\underline{x})$ is the joint probability density function of the defining storm parameters, and $P[\eta(\underline{x}) > \eta]$ is the conditional probability that a storm with the specific characteristics $\underline{x}$ will generate a flood elevation in excess of η (a Heaviside function in the absence of any uncertainties).[2]

In practice, this multiple integral is approximated by a summation over a discrete set of storm-parameter values, as in:

$$P[\eta_{\max(1\,yr)} > \eta] \approx \sum_{i=1}^{n} \lambda_i P[\eta(\underline{x}_i) > \eta] \qquad (2)$$

[2] The right hand side in Equation 1 actually represents the mean annual rate of storms that exceed η at the site, but it also provides a good approximation to the annual exceedence probability when the quantity is small (say, less than 0.1).

where each term in the summation corresponds to one combination of storm parameters (i.e., one synthetic-storm simulation). In its most direct form of implementation, the JPM requires a very great number of such simulations to accurately integrate over the multi-dimensional parameter space (just as the trapezoidal rule may require a very large number of function evaluations to achieve high accuracy). The OS development to be discussed next is a way by which the integration can be accurately achieved with use of a relatively small number of evaluations at a carefully selected set of points (as with ordinary integration using more sophisticated quadrature techniques).

Development of the JPM-OS Method for the Mississippi FEMA Project

The approach followed by the URS team used a Gaussian-process Bayesian quadrature scheme based on the work of Minka (2000), combined with more traditional numerical integration methods. This approach optimizes the selection of the set of storm parameters $\underline{x}_i$ and associated weights p_i (from which the rates $\lambda_i = \lambda p_i$ are computed)[3]. Because the approach makes a number of assumptions regarding the correlation structure of $\eta(\underline{x})$ and because it requires some inputs based on judgment (i.e., the correlation distances associated with the various storm parameters), a number of candidate JPM-OS combinations (which differed in the numbers of synthetic storms and in the values for the correlation distances) were defined and tested against "reference" results that could be considered exact.

A reference case (or 'Gold Standard') was developed for the greater storms, with an extended JPM analysis requiring 2,967 storm simulations using the SLOSH model for the Mississippi coast. The results for the 100-yr and 500-yr surge levels at 147 coastal and inland stations were compared with the results of a series JPM-OS candidates that were also run with the SLOSH model. In this way one of the candidates (designated as JPM-OS 6) was shown to closely replicate the 'Gold Standard' results while requiring only 156 storm simulations.

The storm parameters for the JPM-OS 6 simulation set for the greater storms are given in Table 1. Subsequent simulations of the lesser storms were based on the parameters shown in Table 2.

Each of the greater and lesser synthetic storms was replicated on a number of parallel tracks, described earlier, so that a spatially smooth response estimate would be achieved. Figures 10 and 11 show these tracks near landfall for the greater (152) and lesser storms (76) respectively[4].

Inclusion of the Random Terms

The accuracy of the JPM-OS approach can be improved by accounting for factors that cause variations in the surge response for a given synthetic storm because of effects that are random in nature and not considered in the modeling. The relationship given in Eqn. 2 can be expanded to include these random variations:

$$P[\eta_{\max(1\,yr)} > \eta] \approx \sum_{i=1}^{n} \lambda_i P[\eta(\underline{x}_i) + \varepsilon > \eta] \qquad (3)$$

In this project the random term ε included four components:

ε_1 – represents the astronomical tide level as a random function of the time of landfall. It was evaluated from a two-month tide

[3] See the paper by Toro et al. elsewhere in this volume for a more complete explanation.

[4] Slight differences in track positioning changed the 156 simulations of the SLOSH modeling to the 152 simulations in the final modeling using the PBL-WAM-SWAN-ADCIRC suite.

prediction for Biloxi and has zero mean with a standard deviation of 0.2 m.

ε_2 – represents random variations in the surge response caused by variations of the Holland B parameter. These are random

Table 1. Parameters of JPM-OS 6 scheme for the Greater Storms.

StormID (OWI notation)	dp(mb;coast)	Rp(nmi;offshore)	Vf(m/s)	theta(deg)	Prob.	Annual Rate (each JOS6###% track)
JOS6%	66.69	18.61	6.047	-38.91	1.33E-01	1.32E-03
JOS6%	57.17	39.82	6.047	-13.49	1.20E-01	2.55E-03
JOS6%	49.72	22.93	6.047	-38.92	1.33E-01	1.63E-03
JOS6%	57.17	10.83	6.047	-13.49	1.20E-01	6.94E-04
JOS6%	57.17	20.77	6.047	56.66	1.08E-01	1.19E-03
JOS6%	92.95	14.7	5.943	-12.81	3.42E-02	2.68E-04
JOS6%	78.59	30.8	6.014	-12.82	5.34E-02	8.77E-04
JOS6%	78.59	16.56	4.349	47.33	4.20E-02	3.71E-04
JOS6%	78.59	8.904	6.014	-12.82	5.34E-02	2.54E-04
JOS6%	78.59	16.56	14.54	-12.86	3.49E-02	3.08E-04
JOS6%	70.02	17.98	5.943	-12.82	3.42E-02	3.28E-04
JOS6%	78.59	16.56	4.346	-71.04	4.20E-02	3.71E-04
JOS6%	128.7	11.66	5.943	-12.81	1.06E-02	6.58E-05
JOS6%	103.7	25.3	6.014	-12.82	1.65E-02	2.23E-04
JOS6%	103.7	13.6	4.349	47.33	1.30E-02	9.44E-05
JOS6%	103.7	7.313	6.014	-12.82	1.65E-02	6.44E-05
JOS6%	103.7	13.6	14.54	-12.86	1.08E-02	7.83E-05
JOS6%	94.47	14.53	5.943	-12.82	1.06E-02	8.20E-05
JOS6%	103.7	13.6	4.346	-71.04	1.30E-02	9.43E-05

Notes

1: the Reference storms (e.g., JOS6001) are not assigned any rate. Only JOS6001A, JOS6001B, etc. are used in the probability calculations.

2. The annual rate for each storm is calculated as the storm probability displayed here, times the annual rate of greater storms (2.88E-4 storms/km/yr), times the storm spacing (Rp) in km.

3. The annual rates in column I are the lambda terms in the report text

Table 2. Parameters of JPM-OS Scheme for the Lesser Storms.

StormID (OWI notation)	dp (mb; coast)	Rp (nmi; offshore)	Vf(m/s)	theta (deg)	Prob.	Annual Rate (each *% track)
CAT2001%	46.38	41.59	5.416	8.758	4.74E-02	9.37E-04
CAT2002%	37.75	53.63	2.995	23.55	2.93E-02	7.47E-04
CAT2003%	44.28	21.64	3.4	63.87	7.61E-02	7.83E-04
CAT2004%	40.71	12.72	4.931	-9.324	1.76E-01	1.06E-03
CAT2005%	31.78	44.24	4.881	-11.27	3.92E-02	8.25E-04
CAT2006%	32.11	17.19	6.096	31.22	9.30E-02	7.60E-04
CAT2007%	34.67	24.32	6.941	-71.07	8.75E-02	1.01E-03
CAT2008%	47.53	16.94	4.378	-31.63	6.26E-02	5.04E-04
CAT2009%	42.09	27.82	3.71	-59.19	9.49E-02	1.25E-03
CAT2010%	34.67	24.31	2.458	-5.25	8.75E-02	1.01E-03
CAT2011%	44.28	21.64	10.5	-13.83	7.62E-02	7.83E-04
CAT2012%	37.75	53.63	7.894	-45.75	2.93E-02	7.46E-04
CAT2013%	37.04	29.79	6.644	46.64	1.01E-01	1.44E-03

Notes

1: the Reference storms (e.g., CAT2001) are not assigned any rate. Only CAT2001A, CAT2001B, etc. are used in the probability calculations.

2. The annual rate for each storm is calculated as the storm probability (column H), times the annual rate of storms (2.567E-4 storms/km/yr), times the storm spacing (Rp) in km.

3. The annual rates in column I are the lambda terms in my notes.

variations in the values of B not included in the spatial changes within 90 n.mi. of landfall. This term was evaluated as described in Resio (2007), and is represented by a standard deviation of:

$$\sigma_{\varepsilon_2} = 0.15 * \text{surge elevation} \qquad (4)$$

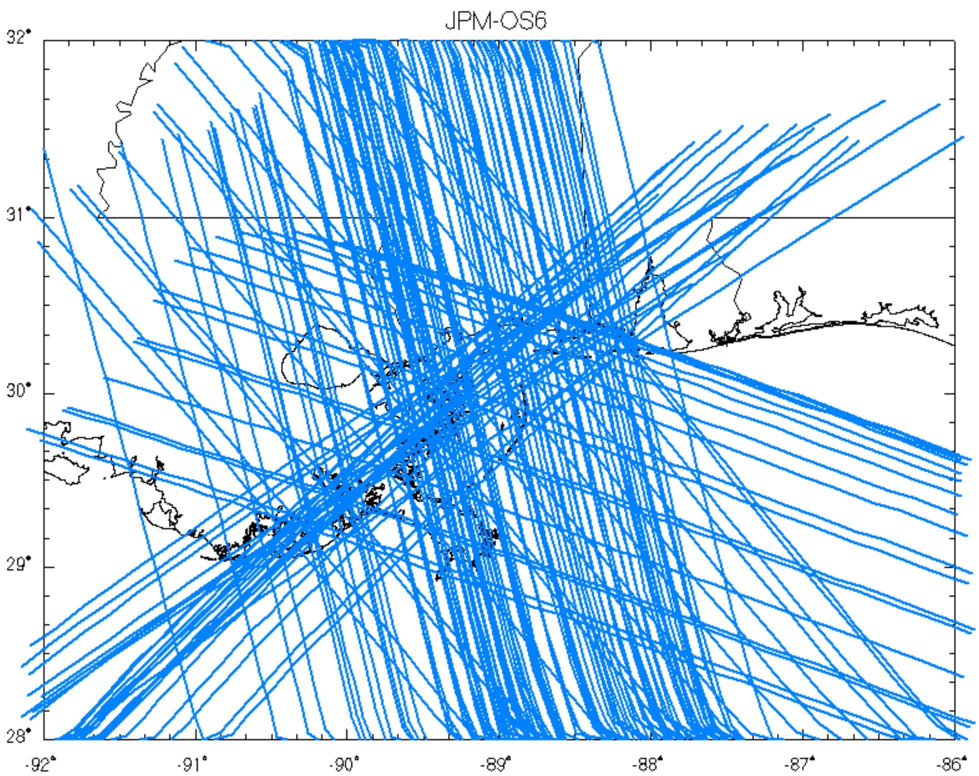

Figure 10. Synthetic storm tracks of the greater storms.

ε_3 – represents random errors in the computed surge caused by lack of skill of the numerical modeling. This was evaluated by comparing values of computed and measured surge at a large number of points for Hurricanes Katrina, Betsy and Camille. It has a standard deviation of 0.23 m.

ε_4 – represents variations in the surge due to a wide range of departures in the real behavior of hurricane wind and pressure fields that are not represented by the PBL model. This was evaluated by comparing the results of surge modeling with hand-crafted 'best winds' compared to the same storms represented only by their major storm parameters with the PBL model. It has a standard deviation of 0.36 m.

These four components are included into Eqn. 3 through a combination defined by:

$$\sigma_{\varepsilon} = \sqrt{\sigma_{\varepsilon_1}^{\ 2} + \sigma_{\varepsilon_2}^{\ 2} + \sigma_{\varepsilon_3}^{\ 2} + \sigma_{\varepsilon_4}^{\ 2}} \qquad (5)$$

Hurricane Surge Simulations

Storm Simulation Work Flow

Each of the 228 synthetic storms was simulated with the model suite consisting of the PBL storm model, the WAM model for waves in the deep Gulf, the SWAN model for nearshore waves and the ADCIRC hydrodynamic model for the computation of the total storm surge. Each of these models was set up and operated on an independent grid so that various interpolations were needed to convert the output from one model to input for the next.

Definitions of the parameter values and tracks for the synthetic storms were developed by Risk Engineering and passed to Oceanweather. OWI operated the PBL model which produced time histories of the corresponding wind and pressure fields. OWI used these results directly as inputs to the WAM model. The results from the PBL and WAM models where then conveyed to the URS team and to the Slinn Group which was responsible for the analysis of wave setup for each storm. For this, the OWI meteorological data were first applied in a reduced version of the ADCIRC model and grid which could be run efficiently on a desktop computer. This model configuration was used to obtain an initial estimate of the time history of water levels during the simulated event. Although this simplified model did not include overland flooding, a reasonable estimate of overland water depths was developed by projecting the height of the coastal surge inland as a level surface. This provided a time series of water depths at the grid points of the SWAN model, extending on land. The SWAN model was driven by a combination of meteorological inputs from the PBL model and deep Gulf wave conditions along an offshore boundary between the WAM and SWAN domains. The output from this modeling phase was an estimate of the radiation stresses during the storm history. These additional stresses, along with the PBL winds and pressures, are applied in a completely new simulation of the storm using the fully-detailed high-resolution ADCIRC model.

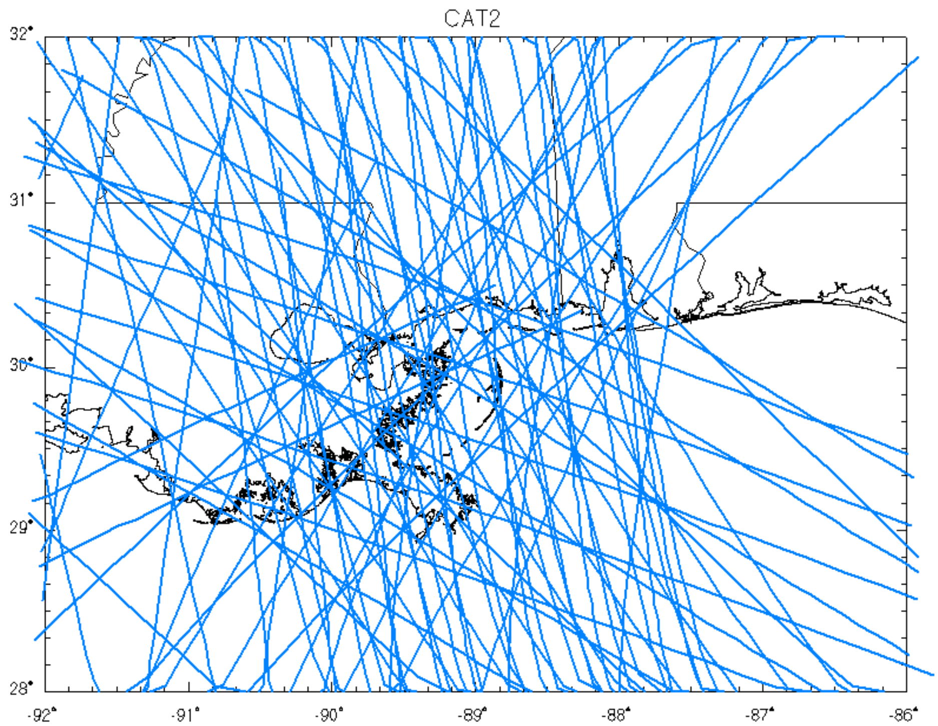

Figure 11. Synthetic storm tracks of the lesser storms.

Hurricane Surge Frequencies

The calculation of still water elevations for given return intervals was made at each of nearly 7,000 output points covering the Mississippi coastal flood plain. At each point, the ADCIRC model simulations provided 228 peak surge heights, each with an associated rate of occurrence.

The results of the 228 individual surges were processed at each point to estimate surge elevations associated with various return intervals. For each point, an initial histogram of the surge levels at a point was generated using 600 bins with an elevation width of 2 cm spanning the range from 0 to 12 meters (above the highest anticipated surge). The rates associated with each simulated storm were accumulated into their appropriate bins. This process yields an approximation of the surge height density distribution at the point, similar to the example shown in Figure 12.

The effect of the composite term ε was then accounted for by redistributing the contents of these bins in a Gaussian pattern over the neighboring bins; the width of the Gaussian redistribution was determined by the sigma associated with the bin. An example of this redistribution is shown in Figure 13, for the contents of a single bin. The result after redistribution of all bins is illustrated in Figure 14. Since a Gaussian has infinite

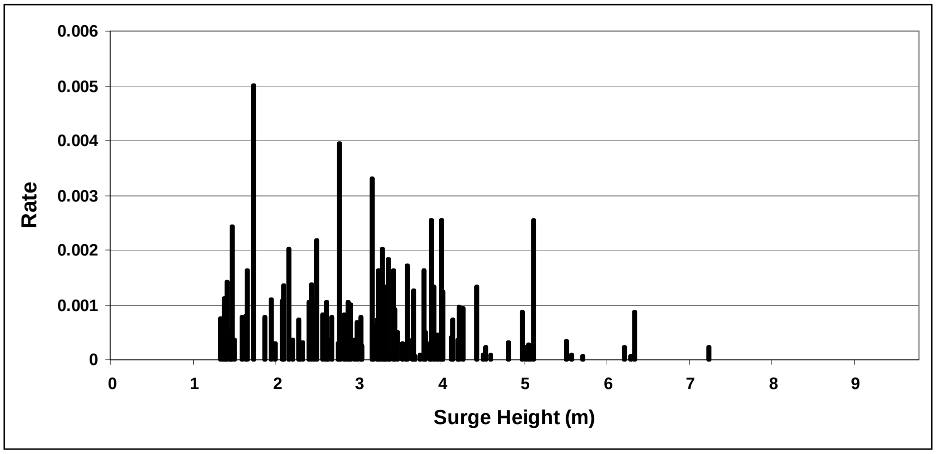

Figure 12. Histogram generated for a single JPM point based on surges and event probabilities.

tails, the small amount of storm rate which would be lost by dispersal beyond the range of the histogram is assigned to the end bins, and total rate is conserved by renormalization as necessary.

The modified histogram was then summed from the highest bin down to the lowest, resulting in an estimate of the cumulative surge distribution, as illustrated in Figure 15. The surge height for any return period can then be interpolated from this curve. For example, the 100-year surge elevation corresponds to a cumulative rate of 0.01 occurrences per year, and is estimated to be about 4.5 meters from the figure. The same procedure yields the 10-, 50-, and 500-year levels, corresponding to cumulative rates of 0.10, 0.02, and 0.002 occurrences per year.

As a final, step the 2%, 1% and 0.2% annual surge levels were compared to the corresponding results from the Corps MsCIP project. They compared acceptably well and were combined so as to produce a single best estimate for the Mississippi coast. The Corps has also been determining coastal flood levels for the adjacent areas of Louisiana, but because of schedule differences those results were not available for final comparisons or for combination.

Wave Heights and Flood Zone Mapping

An additional flood hazard is associated with the waves which ride atop the stillwater elevation determined above. This additional wave crest elevation was determined using FEMA's WHAFIS 4.0 program, following the procedures outlined in FEMA's *Guidelines and Specifications* (FEMA 2003). The wave

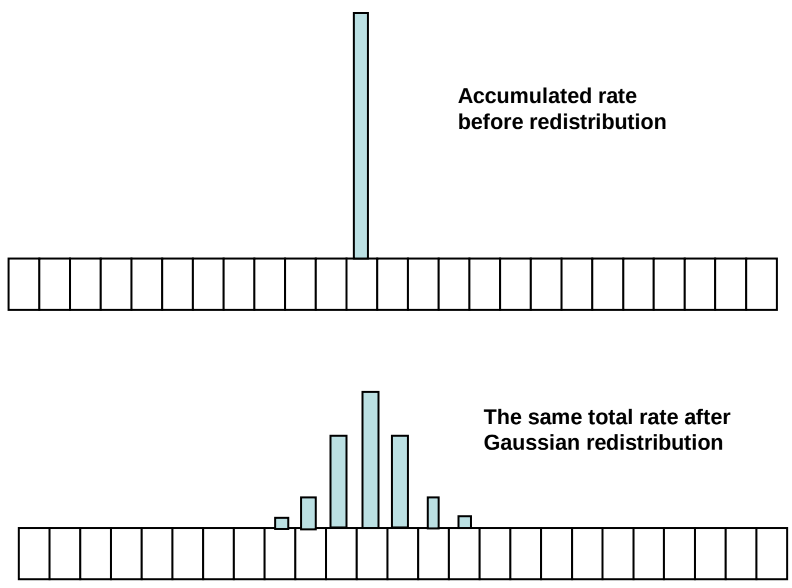

Figure 13. Example of redistribution of the accumulated rate of a single bin to account for secondary random processes.

modeling and subsequent flood zone mapping required multiple high-resolution geospatial datasets, including terrain (topography and bathymetry) and aerial imagery. In this approach, overland wave

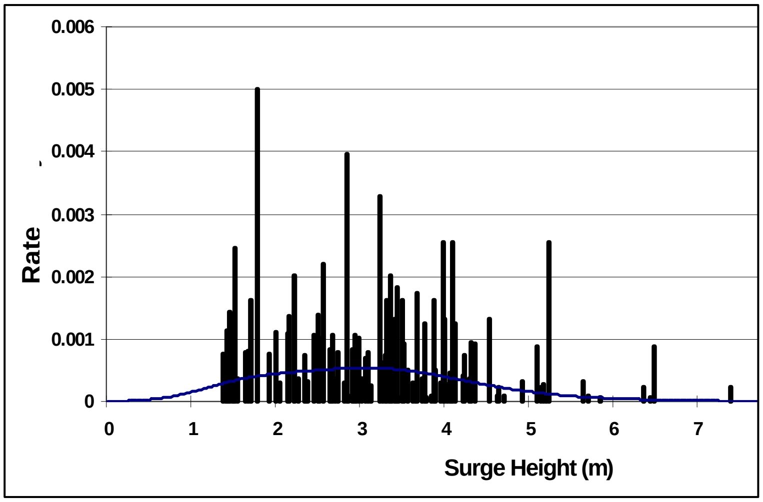

Figure 14. Histogram following the application of the Gaussian redistribution (blue line).

propagation is modeled on a set of transects covering the coastal floodplain in such a way as to represent variations in the features affecting wave propagation, such as vegetation, structures, and open waterways. In all, 161 wave transects were modeled for Jackson, Hancock, and Harrison Counties.

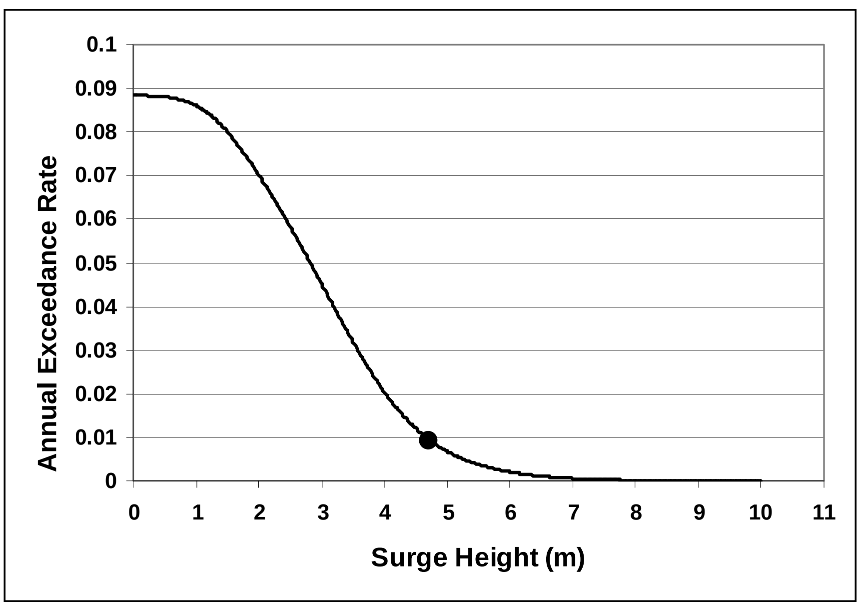

Figure 15. Annual Exceedance Rate and determination of the 100- year surge.

Standard WHAFIS modeling was performed. The computed 100-year flood profiles are subdivided by WHAFIS 4.0 into the regulatory flood hazard zones (VE, AE, and X) and are assigned whole-foot base flood elevations (BFEs). In a small number of cases, the transects crossed slopes steeper than 1:10 for which a wave runup computation was made using the TAW runup model discussed in the FEMA study guidelines. A number of additional specialized GIS tools (including FEMA's CHAMP program, Watershed Concepts' WISE Coastal Module, and the Dewberry GeoFIRM Coastal Tools) were used to translate these zone determinations into the final format required for FEMA digital flood insurance rate maps (DFIRMs).

Acknowledgments

The authors express their appreciation for the extensive discussions and technical exchanges with other members of the URS/FEMA and USACE teams, particularly Vince Cardone, Robert Dean, Leon Borgman, Donald Slinn, Todd Walton, Joannes Westerink, John Atkinson, Lyle Zevenbergen, Andrew Cox, David Levinson, Stephen Baig, Ty Wamsley, Jane Smith, Norm Scheffner, Peter Vickery, and Lynda Charles. It should also be noted that the work on this project was carried out with great dedication by a large team of individuals from the URS Tallahassee and Gaithersburg offices as well from a number of subcontractors including Watershed Concepts and Dewberry. Helpful project and technical management were provided by Dr. Shabbar Saifee and Robert Lowe. Special appreciation is expressed to Richard Sanborn for technical assistance and the preparation of this manuscript. This work was sponsored by FEMA under Contract HSFEHQ-06-J--0018. The opinions expressed here are not necessarily those of the U.S. Government or the sponsoring agency.

References

Blake, E.S., J.D. Jarrell, E.N. Rappaport, and C.W. Landsea, 2006. The Deadliest, Costliest, and Most Intense United States Hurricanes of this Century (And Other Frequently Requested Hurricane Facts), NOAA Technical Memorandum NWS TPC-4.

Borgman, L.E, Miller, M., Butler, L. and R. Reinhard, 1992: Empirical simulation of future hurricane storm histories as a tool in engineering and economic analysis, Proc. Fifth Intn'l, Conf. on Civil Engr. In the Ocean, ASCE, November, College Station, Texas.

Chouinard, L. E. (1992), "A Statistical Method for Regional Design Wave Heights in the Gulf of Mexico," OTC 6832, Proceedings of the Offshore Technology Conference, Houston, TX.

Chouinard, L.M., and C. Liu (1997). "Model for Recurrence Rate of Hurricanes in Gulf of Mexico," *Journal of Waterway, Port, Coastal and Ocean Engineering*, Vol. 123, No. 3, pp. 113-119.

Federal Emergency Management Agency, 2003. *Guidelines and Specifications for Flood Hazard Mapping Partners, Appendix D: Guidance for Coastal Flooding Analyses and Mapping*. Washington, D.C. http://www.fema.gov/plan/prevent/fhm/gs_arch.shtm

Federal Emergency Management Agency, 2007. *Atlantic Ocean and Gulf of Mexico Coastal Guidelines Update*. Washington, D.C. http://www.fema.gov/library/viewRecord.do?id=2458

Goudeau, D.A. and W.C. Conner. Storm Surge Over the Mississippi River Delta Accompanying Hurricane Betsy, 1965". American Meteorological Society, 96:2. (1968).

Hamilton, R.C. and Steere, D.B., 1969, Ocean Gathering Program Report No. 2 Covering Hurricane Camille (17 August 1969), Baylor CO. Consulting Report, Oct. 8, 1969, 27 pps.

Hebert, Paul J., J.D. Jarrell and M. Mayfield, 1996. The Deadliest, Costliest, and Most Intense United States Hurricanes of this Century (And Other Frequently Requested Hurricane Facts), NOAA Technical Memorandum NWS TPC-1.

Ho, F.P., J.C. Su, K.L. Hanevich, R.J. Smith and F.P. Richards, (1987). Hurricane Climatology for the Atlantic and Gulf Coasts of the United States, NOAA Technical Report NWS 38, Silver Spring, MD., April.

Minka, T. P. (2000) Deriving quadrature rules from Gaussian processes, Technical Report, Statistics Department, Carnegie Mellon University. Available on-line at http://research.microsoft.com/~minka/papers/minka-quadrature.ps.gz.

Oceanweather Inc., 2007, Hindcast Wind and Wave Forcing in Support of URS FEMA Mississippi Coastal Flood Map Update, Consulting Report.

Resio, D. (2007). “White Paper on Estimating Hurricane Inundation Probabilities”, Consulting Report prepared by USACE for FEMA.

Scheffner, N., Borgman, L. and D. Mark, 1993: Empirical simulation technique applications to a tropical storm surge frequency analysis of the coast of Delaware, Proc. Third Intn’l Conf. on Estuarine and Coastal Modeling.

Simpson, R.H., Sugg, A. L., Clark, G.B., Frank, N.L., Hope, J.R., Hebert, P.J., Kraft, R.L., and J.M. Pelissier, 1979, The Atlantic Hurricane Season of 1969, Monthly Weather Review, p. 293 – 306.

Toro, G. (2007). “Joint Probability Analysis of Hurricane Flood Hazards for Mississippi”, Consulting Report by Risk Engineering for URS.

Thompson, E.F., and V.J. Cardone, 1996. Practical modeling of hurricane surface wind fields. Journal of Waterway, Port, Coastal, and Ocean Engineering, July/August 1996, pp. 195-205.

Westerink, J.J. and R.A. Luettich, 1991, Tide and storm surge prediction in the Gulf of Mexico using model ADCIRC-2D, Report to the US Army Engineer Waterways Experiment Station, July, 1991.